

Disentangling the surface and bulk electronic states of the Rashba spin-splitting BiTeI

C. Martin,¹ H. Berger,² and D. B. Tanner¹

¹Department of Physics, University of Florida, Gainesville, Florida 32611, USA

²Institute of Physics of Complex Matter, Ecole Polytechnique Fédérale de Lausanne, CH-1015 Lausanne, Switzerland

(Dated: August 29, 2012)

We report the observation of Shubnikov-de Haas (SdH) oscillations in single crystals of the Rashba spin-splitting compound BiTeI, from both longitudinal ($R_{xx}(B)$) and Hall ($R_{xy}(B)$) magnetoresistance. Under magnetic field up to 18 T, we found only one frequency $F = 281 \pm 7$ T, corresponding to a Fermi momentum $k_F \approx 0.1 \text{ \AA}^{-1}$. Angle dependent study strongly suggests that oscillations originate from surface carriers. Combining SdH effect and optical spectroscopy, we demonstrate the existence of two distinct electronic systems: a surface, highly two-dimensional one that give rise to quantum oscillations at lower magnetic field and a second bulk system, that dominates the optical and transport properties.

PACS numbers: 74.25.Ha, 74.78.-w, 78.20.-e, 78.30.-j

The claim of a large Rashba spin-splitting of the bulk electronic bands in BiTeI is based on a combination of theoretical calculations and photoemission spectroscopy (ARPES) [1]. Strong spin orbit interaction, originating from the presence of Bi with its large atomic number, and the absence of a center of inversion in the crystal structure give rise to a significant Rashba term in the Hamiltonian [2], $H_R = \alpha_R (\hat{e}_z \times \vec{k}) \cdot \vec{S}$, where α_R is the Rashba parameter characterizing the strength of the effect, \hat{e}_z is the direction along which the inversion symmetry is broken, \vec{k} represents the momentum, and \vec{S} is the spin of the electrons. The significance of the α_R parameter becomes more clear if we look at the effect of the Rashba term on the energy of a free electron system, which becomes $E_{\pm} = \hbar^2 k^2 / (2m^*) \pm |\alpha_R| k$. The result is that electron energies are split between those with spin up (+) and spin down (-) in a plane perpendicular to \hat{e}_z , as sketched in the upper inset of Fig. 1(a). The momentum and energy splitting both depend on the parameter α_R .

The Rashba effect is of particular interest for the field of spintronics, where one aims to manipulate the spin of electrons for potential applications; moreover, a large value of α_R is very desirable. Values of $\alpha_R \approx 3 \text{ eV\AA}$ were found for asymmetric Bi/Ag(111) interfaces [3, 4]. Recently, Ref. 1 reported an even larger Rashba splitting, $\alpha_R = 3.8 \text{ eV\AA}$, in the bulk electronic bands of BiTeI. Optical spectroscopy of this compound found indeed an electronic excitation spectrum consistent with the splitting of the bulk conduction and valence bands [5] and further photoemission study suggested the 3D nature of these bands [6]. More recent ARPES reports however, indicated the reconstruction of the band structure at the Te (or I) terminated surface and the existence of surface electronic branches, possibly with even larger Rashba spin-splitting [7, 8]. On the theoretical side, *ab-initio* calculations for BiTeX (X=Cl, Br, I) do claim the formation of a surface 2D electron system distinct from the bulk states that has a larger Rashba splitting [9].

Given that the fate of the surface states in BiTeI is still a

debated issue and noting the particular sensitivity of photoemission experiments to the surface, we measured the in-plane longitudinal magnetoresistance $R_{xx}(B)$ and transverse (Hall) resistance $R_{xy}(B)$ in single crystals of BiTeI, searching for Shubnikov-de Haas oscillations as an alternative route to investigate the Fermi surface. Furthermore, we combine the results with optical reflectance data to disentangle the electronic properties of bulk and surface carriers.

Single crystals of BiTeI were grown by chemical vapor transport and Bridgman method. Two samples were initially screened and both revealed very similar quantum oscillations. Then, a complete study was performed on one sample with approximate dimensions $4 \times 6 \times 0.09 \text{ mm}^3$. Gold wires were attached using silver paint and sample resistance was measured using a commercial resistance bridge. The experiment was performed in the SCM-2 facility at the National High Magnetic Field in Tallahassee. The facility consists of a top loading ^3He cryostat, with sample in liquid and a base temperature of 0.3 K, and an 18–20 Tesla superconducting magnet. Samples were mounted on a rotating probe with an angular resolution better than 1° . Optical reflectance measurements were performed at the University of Florida. The data for frequencies between 30 and 5000 cm^{-1} (4–620 meV), at temperatures as low as 10 K, were obtained using a helium flow cryostat mounted on a Bruker 113v Fourier spectrometer. Higher frequency reflectance, up to $\omega \approx 30000 \text{ cm}^{-1}$ was measured at room temperature with a Zeiss microscope photometer and used to extrapolate the 10 K data for Kramers-Kronig analysis.

Main panel of Fig. 1(a) shows the high magnetic field behavior of R_{xx} at 0.3 K, plotted against inverse field. A small modulation, periodic in $1/B$ can be directly observed in the figure. Moreover, we also found oscillations with the same frequency in the transverse resistance R_{xy} . Although these may be difficult to see in the main panel of Fig. 1(b), due to a large Hall coefficient, the oscillatory behavior of the Hall resistance becomes obvious in the inset, where we plot $dR_{xy}/dB(B)$. A Fourier transform of these data yields a frequency of oscillations $F = 281 \pm 7$ Tesla

for the field applied normal to the sample surface. This frequency is directly proportional to the area of the Fermi surface $S_F = 2\pi eF/\hbar$ and furthermore to the Fermi momentum $k_F = (S_F/\pi)^{1/2} = 0.092 \pm 0.001 \text{ \AA}^{-1}$. Notably, this value of k_F is comparable to that from some of the Fermi surfaces observed in photoemission experiments; it is nearly identical to the results from Ref. 1 and 6, which assign it to a bulk conduction branch and agrees within 50% with the values from Ref. 8, but for the surface electronic bands. Moreover, it also agrees within better than 50% with the value of k_F for the surface states near the bottom of the conduction band, obtained from band structure calculations [9].

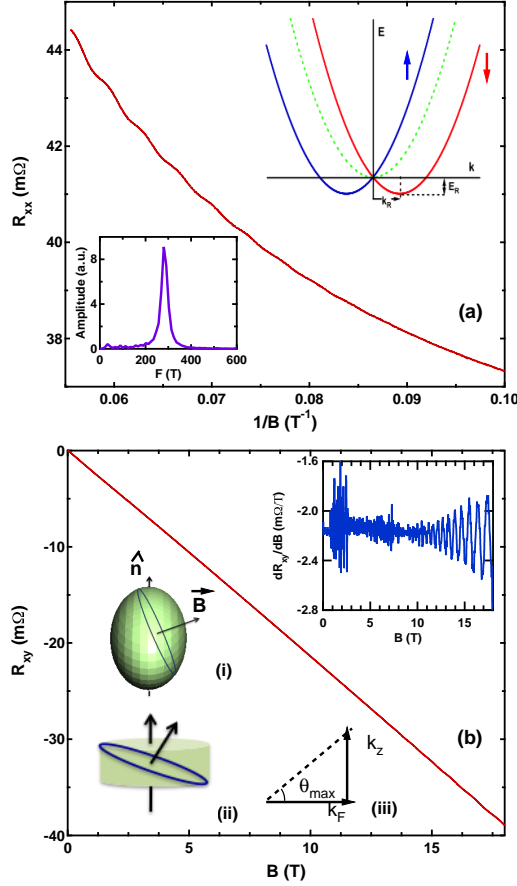


FIG. 1. (Color online) (a) Main panel: Longitudinal resistance R_{xx} vs. $1/B$ at $T = 0.3$ K for the magnetic field applied normal to sample surface. Upper inset: 1D representation of a Rashba spin-split conduction band showing the momentum (k_R) and the energy (E_R) splits. Lower inset: Fourier Transform of $R_{xx}(1/B)$. (b) Main panel: $R_{xy}(B)$. Upper inset: The field derivative of $R_{xy}(B)$, showing the presence of SdH oscillations at high magnetic field. The large noise between 1 and 3 T is due to magnetic flux jumps in the superconducting magnet. Lower inset: (i) Sketch of electron orbit in a tilted magnetic field for a 3D Fermi surface. (ii) Same for a thin 2D cylindrical Fermi surface. (iii) Geometrical representation of a maximum tilt angle above which electron orbits of a surface electron system become open.

The angular dependence of the SdH oscillations provides a valuable insight into the dimensionality of the Fermi surface. A 3D Fermi surface always has closed electron orbits, and thus oscillations should be, in principle, observed for any angle between the magnetic field and sample surface. (See inset (i) of Fig. 1(b)). A quasi-2D Fermi surface (e.g., a cylinder) would show oscillations up to relatively large angles, provided that their frequency can be measured with the highest available magnetic field. In contrast, a strictly 2D layer backed by a conducting bulk may lose orbital coherence if a tilted field drives carriers into the bulk (inset (ii) of Fig. 1(b)).

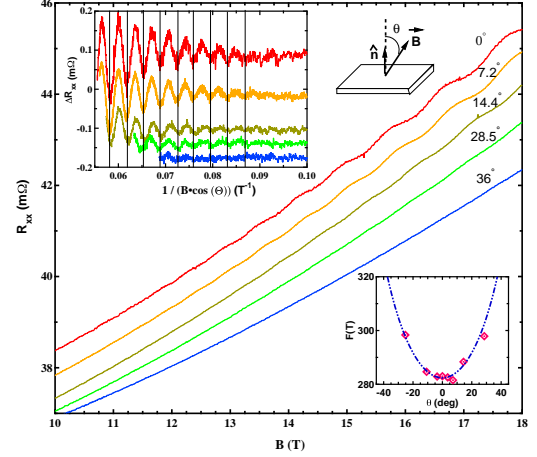


FIG. 2. (Color online) Main panel: $R_{xx}(B)$ above 10 T for different angles between the magnetic field and the sample surface. Upper inset: ΔR_{xx} vs. the magnetic field component along the normal to sample surface and a sketch of the sample in tilted magnetic field. Lower inset: Angle dependence of the oscillation frequency (symbols) and fit to $1/\cos(\theta)$ (dashed line).

The main panel of Fig. 2 shows the high magnetic field behavior (above 10 T) of R_{xx} for different angles θ between the field and the sample surface, like sketched in the upper right inset. It can be visually observed that the oscillations are rapidly suppressed with increasing θ and that they are absent above $\theta \approx 30^\circ$. The angular dependence of their frequency, shown in the lower inset of Fig. 2, has a $1/\cos(\theta)$ behavior, indicating a 2D character of the Fermi surface, whether it corresponds to bulk or surface electrons. The origin of this Fermi surface becomes more clear if we look at ΔR_{xx} , obtained after background subtraction, in the upper inset of Fig. 2. First, we notice again the rapid decrease of oscillation amplitude with the angle of the magnetic field. Although not shown here, we measured up to $\theta > 90^\circ$, rotating the sample both directions with respect to the magnetic field and we confirm that oscillations only exist for $|\theta| \leq 30^\circ$. Second, we see that their period scales remarkably well with the component of magnetic field perpendicular to the sample surface ($1/B \cdot \cos(\theta)$). These observations provide strong indication that the oscillations originate from surface carriers rather than from

the bulk, similar to the results obtained from surface carriers of 2D structures [10] and of some of the topological insulators [11].

The surface carrier concentration (for two spin components) can now be written as a function of the SdH frequency: $n_{2D} = eF/(\pi\hbar)$, and we obtain $n_{2D} = 1.4 \times 10^{13} \text{ cm}^{-2}$. At least hypothetically, we can estimate the thickness of the surface electron system. Considering a cylindrical Fermi surface with a small height k_z in momentum space, the orbit of electrons in an applied magnetic field will become open, no longer giving rise to quantum oscillations, at an extreme angle θ_{max} , so that $k_z = 2k_F \tan(\theta_{max})$. (See inset (iii) of Fig. 1(b).) Assuming a $\theta_{max} \approx 40^\circ$, and the value of k_F from above, we obtain $k_z \approx 0.15 \text{ \AA}^{-1}$. Then, the thickness of the surface electronic system $t = 1/k_z$ is estimated to $t \approx 6.5 \text{ \AA}$, very close to the height of one unit cell $c = 6.85 \text{ \AA}$, obtained from X-ray diffraction [12, 13].

Therefore, these data strongly suggest the existence of a 2D surface electron system within the top unit cell of BiTeI, in agreement with the conclusion of recent band structure calculations [9]. We also propose that the split branch with $k_F \approx 0.1 \text{ \AA}^{-1}$ observed in ARPES experiments corresponds to surface states, more in line with the conclusion of Refs. 7 and 8. It is also worth mentioning that some photoemission reports suggests a 3D character of the bulk electronic branches [6], which would be contrary to our finding if the oscillations observed in our study were to originate from bulk.

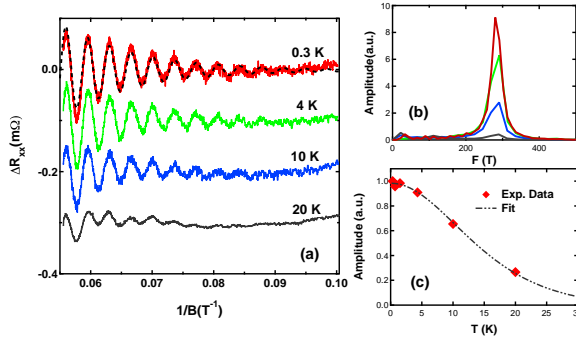


FIG. 3. (Color online) (a) ΔR_{xx} vs. $1/B$ (with B above 10 T and applied perpendicular to the sample surface) at temperatures from 0.3 to 20 K. The dashed line is a fit of the data at 0.3 K to the expression: $\exp(-\gamma T_D) \cos(2\pi F/B + \pi)$ as explained in the text. (b) Fourier transform of the data from panel (a). (c) Amplitude of oscillations at $1/B = 0.06 \text{ T}^{-1}$ for different temperatures, normalized to the value at 0.3 K (symbols) and a fit to the temperature-dependent damping term $\gamma T/\sinh(\gamma T)$, as explained in the text (dot-dash line).

To investigate further the properties of these surface electrons, we measured the temperature and magnetic-field dependence of the quantum oscillations. Figure 3(a) shows the resistance ΔR_{xx} (after background subtraction) versus inverse field at different temperatures. Oscillations are

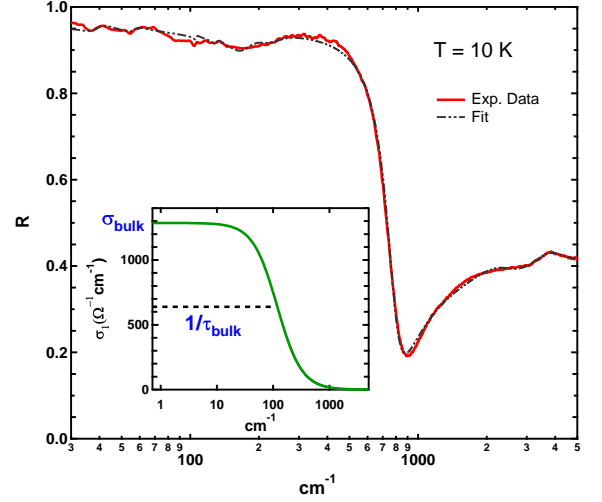


FIG. 4. (Color online) Main panel: $\mathcal{R}(\omega)$ at $T = 10 \text{ K}$ (continuous red line) and a Drude-Lorentz fit (dashed dotted black line). Inset: Real part of optical conductivity obtained from the Lorentz-Drude fit, from which the bulk DC conductivity and the scattering rate of the bulk carriers are obtained.

visible up to at least 20 K, although significantly damped due to the thermal broadening of the quantized Landau levels. The effect of temperature is also evident if we look at the amplitude of the Fourier transform shown in Fig. 3(b). This quantity is expected to follow the Lifshitz-Kosevich temperature dependence, $\gamma T/\sinh(\gamma T)$, with $\gamma = 14.69 m^*/m_0 B$, where B is the magnetic field, m^* is the effective mass, and m_0 the rest mass of the electron [14]. Figure 3(c) shows that result of the fit to the above expression for the amplitude at $1/B = 0.06 \text{ T}^{-1}$, which gives $m_s^* = 0.18 m_0$.

At fixed temperature, the amplitude of the SdH oscillations is enhanced by increasing field (decreasing $1/B$) as $\Delta R_{xx} \propto \exp(-\gamma T_D) \cos(2\pi F/B + \pi)$, where γ is defined above and T_D is the Dingle temperature, $T_D = \hbar/(2\pi\tau k_B)$, related to the lifetime τ of electrons [14]. In Fig. 3(a) we show the fit of the data at 0.3 K, where it can be seen that both the amplitude and the phase are well reproduced by only considering one frequency. We obtain a Dingle temperature $T_D = 31 \text{ K}$, which in turn gives a lifetime $\tau_s = 4 \times 10^{-14} \text{ s}$, for the surface carriers. Now, we estimate the surface mobility $\mu_s = e\tau_s/m_s^* \approx 400 \text{ cm}^2/(\text{V}\cdot\text{s})$ and the sheet conductance (resistance) $G_{\square} \approx 10^{-3} \Omega^{-1}$ ($R_{\square} \approx 1 \text{ k}\Omega$). The properties obtained for the surface carriers are summarized in Table I.

Further characterization of the electronic properties of BiTeI requires a technique complementary to SdH oscillations; one that mostly probes the bulk. Optical reflectance is a very suitable tool. The main panel of Fig. 4 shows the optical reflectance spectrum $\mathcal{R}(\omega)$ of the same sample at $T = 10 \text{ K}$. The data are similar to a previous optical study [5]: there are several features at low frequency asso-

TABLE I. Parameters of the bulk and surface carriers

	Surface	Bulk
σ	$10^{-3} \Omega^{-1}$	$1300 \Omega^{-1} \text{cm}^{-1}$
μ ($\text{cm}^2/\text{V}\cdot\text{s}$)	400	150
τ (s)	4×10^{-14}	4.5×10^{-14}
m^*/m_0	0.18	0.5
n	$1.4 \times 10^{13} \text{cm}^{-2}$	$5.8 \times 10^{19} \text{cm}^{-3}$

ciated with lattice vibrations, a clear sharp plasma edge at about 850 cm^{-1} ($\approx 0.1 \text{ eV}$) and broad structure at higher frequencies due to interband transitions.

This reflectance is dominated by the bulk carriers. We may estimate the contribution of the surface electrons to $\mathcal{R}(\omega)$. The surface carriers contribute an impedance mismatch, but this surface impedance is $R_{\square} \approx 1 \text{ k}\Omega$. A free-standing thin film with this impedance has a reflectance of $\mathcal{R} = (Z_0/R_{\square})^2 / (2 + Z_0/R_{\square})^2 \approx 0.02$, where $Z_0 = 377 \Omega$ is the vacuum impedance [15]. However, we see in Fig. 4 that at low frequencies $\mathcal{R}(\omega) \approx 0.96$. Also, a few Angstrom-thick layer with a surface impedance of $R_{\square} \approx 1 \text{ k}\Omega$ would only attenuate the incident light by about 1% in the frequency range of our measurements. Simulations show that for a conducting bulk (as we find below) the addition of the monolayer-thick conducting surface layer changes the reflectance by less than 0.5% (see supplemental information). Therefore, most of the light probes the bulk.

Analysis of optical reflectance [16] may use either Kramers-Kronig transformation or fits to a model such as the Drude-Lorentz model in order to estimate other optical quantities, such as the optical conductivity $\sigma(\omega)$. Here we have fit $\mathcal{R}(\omega)$ with the Drude-Lorentz model and the result is shown in Fig. 4 as the dash-dot line. The corresponding Drude contribution to the conductivity $\sigma_1(\omega) = \sigma_b / (1 + \omega^2 \tau_b^2)$ is shown in the inset. (The Kramers-Kronig-derived conductivity is very similar.) The lattice vibrations and interband transitions seen in Fig. 4 will be discussed in a separate work, here we focus on the free-carrier contribution to $\sigma_1(\omega)$. From the fit we obtain the scattering rate $1/\tau_b = 118 \pm 5 \text{ cm}^{-1}$ ($\tau_b \approx 4.5 \times 10^{-14} \text{ s}$), the plasma frequency $\omega_p = 3030 \text{ cm}^{-1}$ ($\approx 6 \times 10^{14} \text{ rad/s}$) and, hence, the bulk conductivity $\sigma_b = 1300 \pm 80 \Omega^{-1} \text{cm}^{-1}$.

It is worth noticing that the sheet conductance associated with the bulk would be, for our sample thickness of $d = 85 \pm 15 \mu\text{m}$, $G_{b\square} \approx 10 \Omega^{-1}$ ($R_{b\square} \approx 0.1 \Omega$). The bulk conductance is four orders of magnitude larger than the surface conductance, implying that most of the transport properties are dominated by the bulk carriers. We may therefore use the Hall resistance to determine the bulk carrier concentration. In Fig. 1(b), from a direct fit of the low field region, we find the slope $(dR_{xy}/dB) = R_H/d = -2.1 \text{ m}\Omega/\text{T}$, where $R_H = 1/(n_b e)$ is the Hall coefficient and d is sample thickness given above. The negative sign indicates that carriers are electrons. Hence, the bulk

carrier concentration is $n_b = (5.8 \pm 1.0) \times 10^{19} \text{ cm}^{-3}$. Based on this value, we estimate that quantum oscillations originating from the bulk should have a frequency $F \approx 580 \text{ T}$ (not accounting for the Rasba spin-splitting), which is about twice the value that we attribute to the surface. The likely reason for not detecting this additional frequency in the Shubnikov-de Haas effect is the lower mobility of the bulk carriers. From the plasma frequency $\omega_p = n_b e^2 / (m_b^* \epsilon_0)$, where ϵ_0 is the free space permittivity, the bulk effective mass is $m_b^* \approx 0.5 m_0$, which is almost three times larger than that of the surface carriers. As a consequence, given that the scattering rates obtained earlier are very similar (see Table 1), the obtained bulk mobility $\mu_b = e\tau_b/m_b^* \approx 150 \text{ cm}^2/(\text{V}\cdot\text{s})$ is almost three times smaller than that of the surface. Therefore, it would require about three times larger magnetic field to detect quantum oscillations from the bulk carriers. The carrier parameters are summarized in Table I.

In conclusion, we have established the existence of surface electronic states in BiTeI from Shubnikov-de Haas oscillations. Combining with optical spectroscopy, we fully resolve the electronic properties of both surface and bulk carriers (Table 1). We found that, while the scattering rates are very similar, the surface carriers are almost three times lighter, therefore they have almost three times higher mobility.

A portion of this work took place at the University of Florida, supported by the DOE through Grant No. DE-FG02-02ER45984. A portion was performed at the National High Magnetic Field Laboratory, which is supported by National Science Foundation Cooperative Agreement No. DMR-0654118, the State of Florida, and the U.S. Department of Energy. We would also like to thank Ju-Hyun Park, Glover Jones, and Timothy Murphy for support with the experiment at the National High Magnetic Field Laboratory. We also thank Dmitrii Maslov for stimulating discussions.

-
- [1] K. Ishizaka, M. S. Bahramy, H. Murakawa, M. Sakano, T. Shimojima, T. Sonobe, K. Koizumi, S. Shin, H. Miyahara, A. Kimura, K. Miyamoto, T. Okuda, H. Namatame, M. Taniguchi, R. Arita, N. Nagaosa, K. Kobayashi, Y. Murakami, R. Kumai, Y. Kaneko, Y. Onose, Y. Tokura, *Nature Materials*, **10**, 521 (2011).
 - [2] E. I. Rashba, *Sov. Phys. Solid State*, **2**, 1109–1122 (1960).
 - [3] Yu. M. Koroteev, G. Bihlmayer, J. E. Gayone, E. V. Chulkov, S. Blügel, P. M. Echenique and Ph. Hofmann, *Phys. Rev. Lett.*, **93**, 046403 (2004).
 - [4] C. R. Ast, J. Henk, A. Ernst, L. Moreschini, M. C. Falub, D. Pacil, P. Bruno, K. Kern, M. Grioni, *Phys. Rev. Lett.*, **98**, 186807 (2007).
 - [5] J. S. Lee, G. A. H. Schober, M. S. Bahramy, H. Murakawa, Y. Onose, R. Arita, N. Nagaosa, Y. Tokura, *Phys. Rev. Lett.*, **107**, 117401 (2011).

- [6] M. Sakano, J. Miyawaki, A. Chainani, Y. Takata, T. Sonobe, T. Shimojima, M. Oura, S. Shin, M. S. Bahramy, R. Arita, N. Nagaosa, H. Murakawa, Y. Kaneko, Y. Tokura, K. Ishizaka, *arxiv:1205.3005*, (2012). (unpublished)
- [7] G. Landolt, S. V. Ereameev, Y. M. Koroteev, B. Slomski, S. Muff, M. Kobayashi, V. N. Strocov, T. Schmitt, Z. S. Aliev, M. B. Babanly, I. R. Amiraslanov, E. V. Chulkov, J. Osterwalder, J. H. Dil, *arxiv:1204.2196*, (2012). (unpublished)
- [8] A. Crepaldi, L. Moreschini, G. Auts, C. Tournier-Colletta, S. Moser, N. Virk, H. Berger, Ph. Bugnon, Y. J. Chang, K. Kern, A. Bostwick, E. Rotenberg, O. V. Yazyev, M. Grioni, *arxiv:1205.1395*, (2012). (unpublished)
- [9] S. V. Ereameev, I. A. Nechaev, Y. M. Koroteev, P. M. Echenique, E. V. Chulkov, *arxiv:1205.2006* (2012). (unpublished)
- [10] A. D. Caviglia, S. Gariglio, C. Cancellieri, B. Sacépé, A. Fête, N. Reyren, M. Gabay, A. F. Morpurgo, J.-M. Triscone *Phys. Rev. Lett.*, **105**, 236802 (2010).
- [11] J. G. Analytis, R. D. McDonald, S. C. Riggs, J. H. Chu, G. S. Boebinger, I. R. Fisher *Nature Physics*, **6**, 960–964 (2010).
- [12] A. Tomokiyo, T. Okada, S. Kawano, *Jpn. J. Appl. Phys.*, **16**, pp. 291-298 (1977).
- [13] A. V. Shevelkov, E. V. Dikarev, R. V. Shpanchenko, B. A. Popovkinet, *Journal of Solid State Chemistry*, **114**, 379-384 (1995).
- [14] D. Shoenberg, *Magnetic Oscillations in Metals* (Cambridge University Press, Cambridge, 1984).
- [15] L. H. Palmer, M. Tinkham, *Phys. Rev.*, **165**, 588–595 (1968).
- [16] F. Wooten, *Optical Properties of Solids* (Academic Press, Inc., 1972).